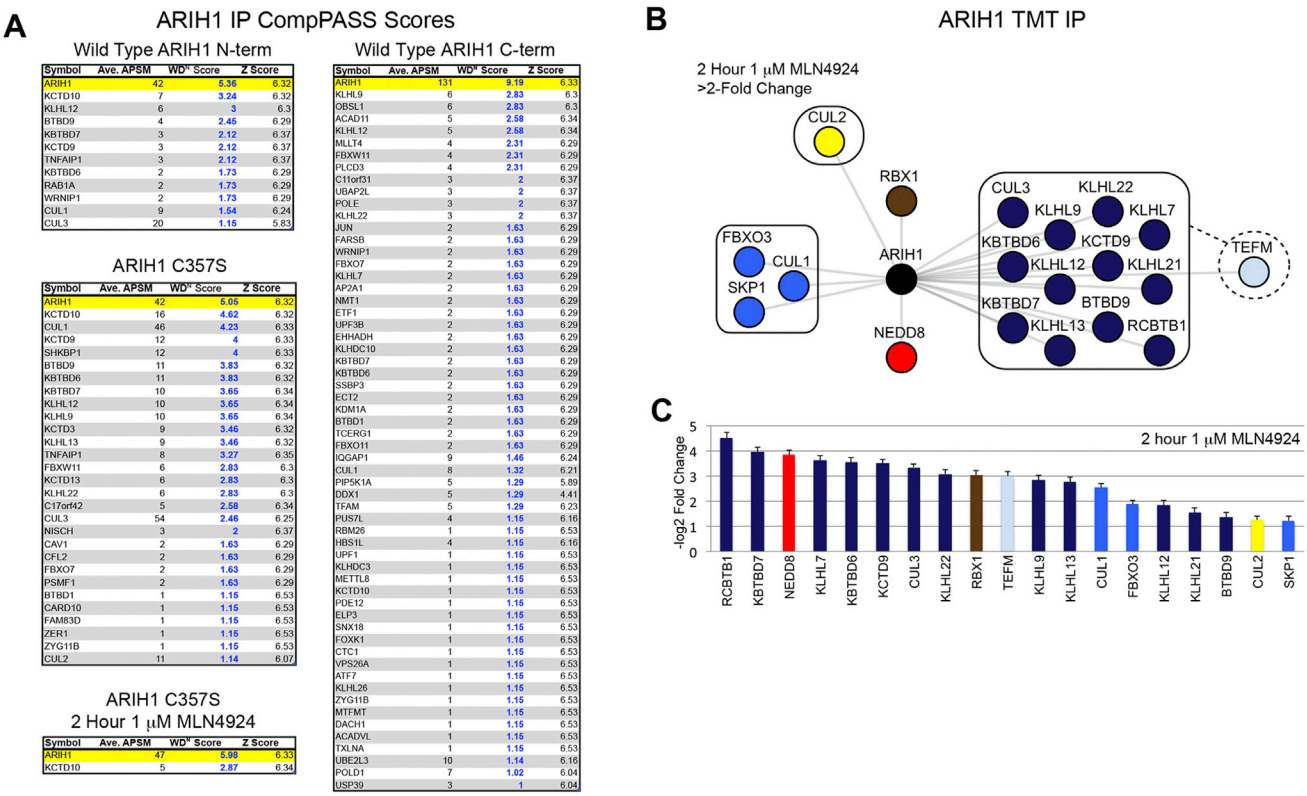

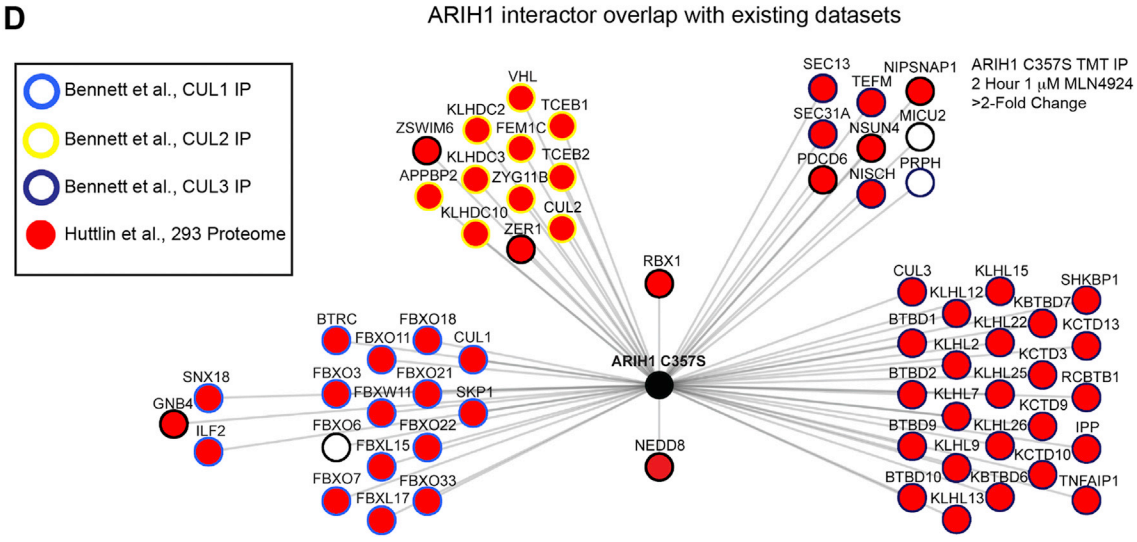

Figure S1. Proteomic Identification of ARIH1-Interacting Proteins Reveals Widespread Connections to Active CRLs, Related to Figure 1

(A) CompPASS analysis scores for High Confidence candidate Interacting Proteins (HCIPs) identified from immune complexes with ARIH1 and ARIH1^{C357S} in 293T cells.

(B) Schematic from TMT Affinity-Purification and Mass spectrometry (AP-MS) quantification of NEDD8-dependent interacting partners of wild-type ARIH1, showing interacting proteins with greater than a 2-fold change following a 2 hr MLN4924 treatment. CUL1 and a known F-box protein SR are labeled in blue, CUL3 and its SRs in purple, RBX1 in brown, NEDD8 in red, and another previously described CRL-associated protein in light blue.

(C) Log2 fold change of WT ARIH1 interactors from the schematic in panel B. Error bars: ± SE.

(D) Summary of ARIH^{C357S} interactors compared to those identified in CUL1, CUL2, or CUL3 immune complexes or found in the 293T proteome in previous studies (Bennett et al., 2010; Huttlin et al., 2015).

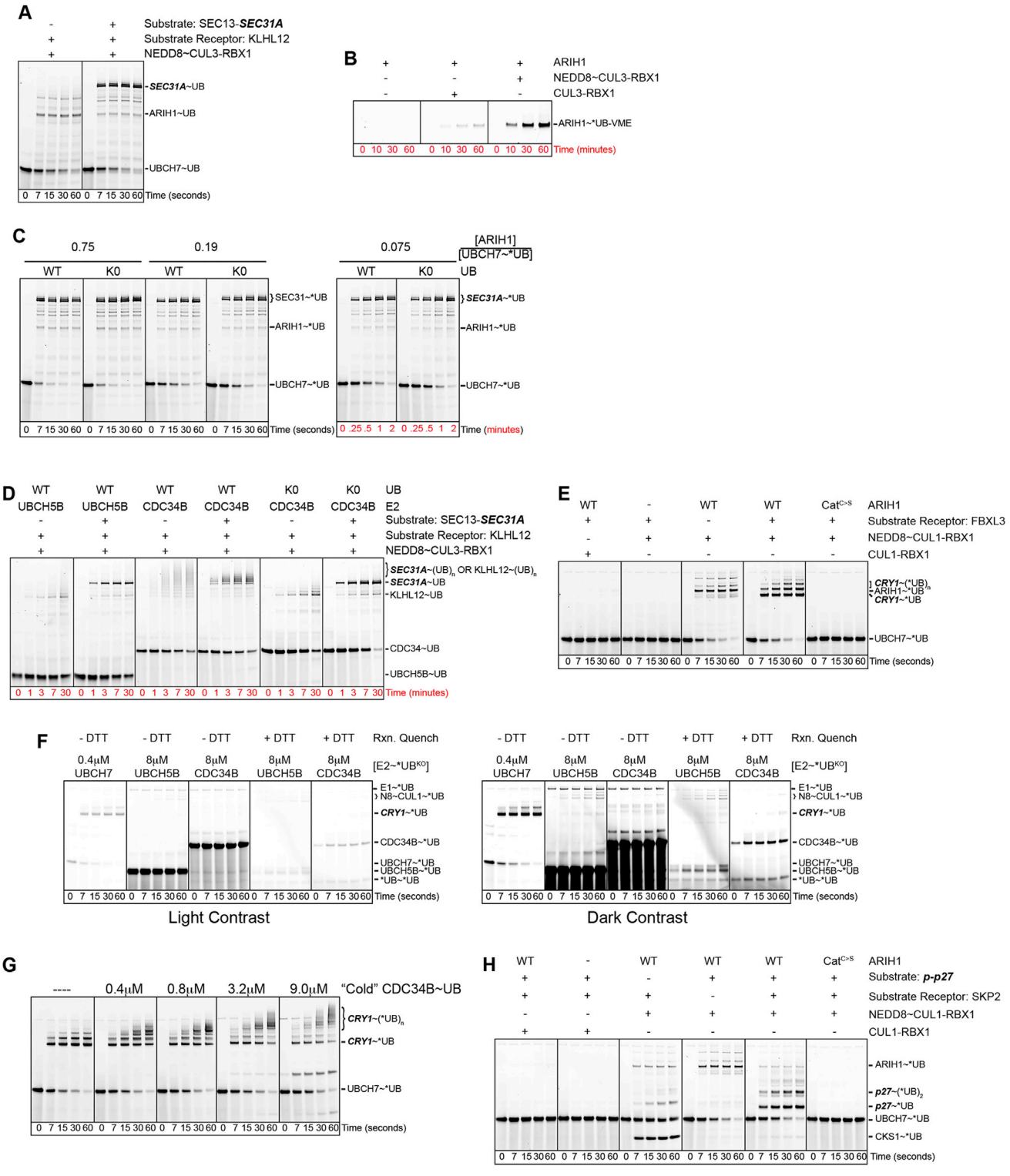

Figure S2. Controls Comparing the ARIH1 RBR-CRL and Conventional CRL RING-E2 Mechanisms for UB Targeting to CRL Client Substrates, Related to Figure 2

(A) All lanes contain UBCH7 and ARIH1. Pulse-chase assay monitors *UB transfer from thioester-linked UBCH7∼*UB intermediate via ARIH1 in the absence or presence of SEC13-SEC31A. In the absence of substrate, when activated by neddylated CUL3–RBX1, ARIH1 primarily auto-modifies itself even in the presence of KLHL12.

(legend continued on next page)

(B) Monitoring the reactivity of ARIH1's catalytic cysteine with *UB-VME probes for "Opening" of the autoinhibited structure. Experiments test ARIH1 reaction with *UB-VME in the absence of CUL3–RBX1, or in the presence of non-neddylated or neddylated CUL3–RBX1, demonstrating the requirement for cullin neddylation to relieve autoinhibition and stimulate ARIH1 opening to expose the catalytic Cys.

(C) Assays as in panel A compare *UB and *UB K0 transfer to SEC31A via ARIH1/UBCH7 while systematically reducing the ratio of ARIH1 to UBCH7∼*UB to test ARIH1's preference for mono or polyubiquitylation of CRL substrates. Lower ARIH1:UBCH7∼*UB ratios ensure ARIH1 must engage in multiple catalytic cycles to deplete the starting pool of *UB∼UBCH7. With each cycle, *UB∼UBCH7–ARIH1 would increasingly confront more *UB-modified SEC31A that could in principle serve as a substrate for UB chain elongation. However, even with ≈10-fold less ARIH1, the reaction profiles look identical with WT or K0 *UB. This contrasts with the reaction with CDC34, where a neddylated CRL and CDC34 preferentially elongate UB chains on the small fraction of ubiquitylated substrate. The data are consistent with the ARIH1–neddylated CRL pathway preferentially mediating monoubiquitylation, on multiple sites in the case of SEC31A, of a CRL substrate.

(D) Pulse-chase assay monitoring *UB or *UB K0 transfer through the conventional RING–E2 pathway by neddylated $CRL3^{KLHL12}$ with either UBCH5B or CDC34 as E2, in the absence or presence of the substrate SEC13-SEC31A. In the absence of substrate the conventional pathway targets the SR KLHL12 at extended time points of the chase. Note the duration of the chase in this assay proceeds for 30 min to further demonstrate differences between the ARIH1–CRL (Panel A, 60 s time-course) and the conventional mechanisms.

(E) Substrate receptor used in these reactions is FBXL3. Side-by-side assays testing dependence of substrate receptor, CUL1 neddylation, and ARIH1's catalytic cysteine for ARIH1–neddylated CRL-mediated UB transfer to the substrate CRY1. Pulse-chase assay monitors the transfer of *UB from UBCH7 via ARIH1.

(F) Pulse-chase assays starting with indicated E2 ∼*UB K0 compare neddylated $CRL1^{FBXL3}$-mediated modification of substrate CRY1 via ARIH1–CRL pathway using UBCH7∼*UB at concentrations shown in Figure 3C, or with 20-fold higher concentrations of the E2s UBCH5B or CDC34B in the canonical CRL RING mechanism. Gels were run side-by-side and identical light (left) or dark (right) contrasts are shown for comparison of product formation with the different concentrations of starting E2 ∼*UB.

(G) Pulse-chase assays monitor fate of CRY1 marked with fluorescent *UB via UBCH7∼*UB/ARIH1/neddylated $CRL1^{FBXL3}$ in the absence or presence of the indicated concentrations of unlabeled CDC34∼UB. The data suggest that the $CRL1^{FBXL3}$ substrate CRY1 could be rapidly modified by > 10 UBs the presence of both the ARIH1 pathway and saturating CDC34∼UB.

(H) Same as (E) except with the F-box protein SKP2 as the substrate receptor and phospho-p27 as the substrate.

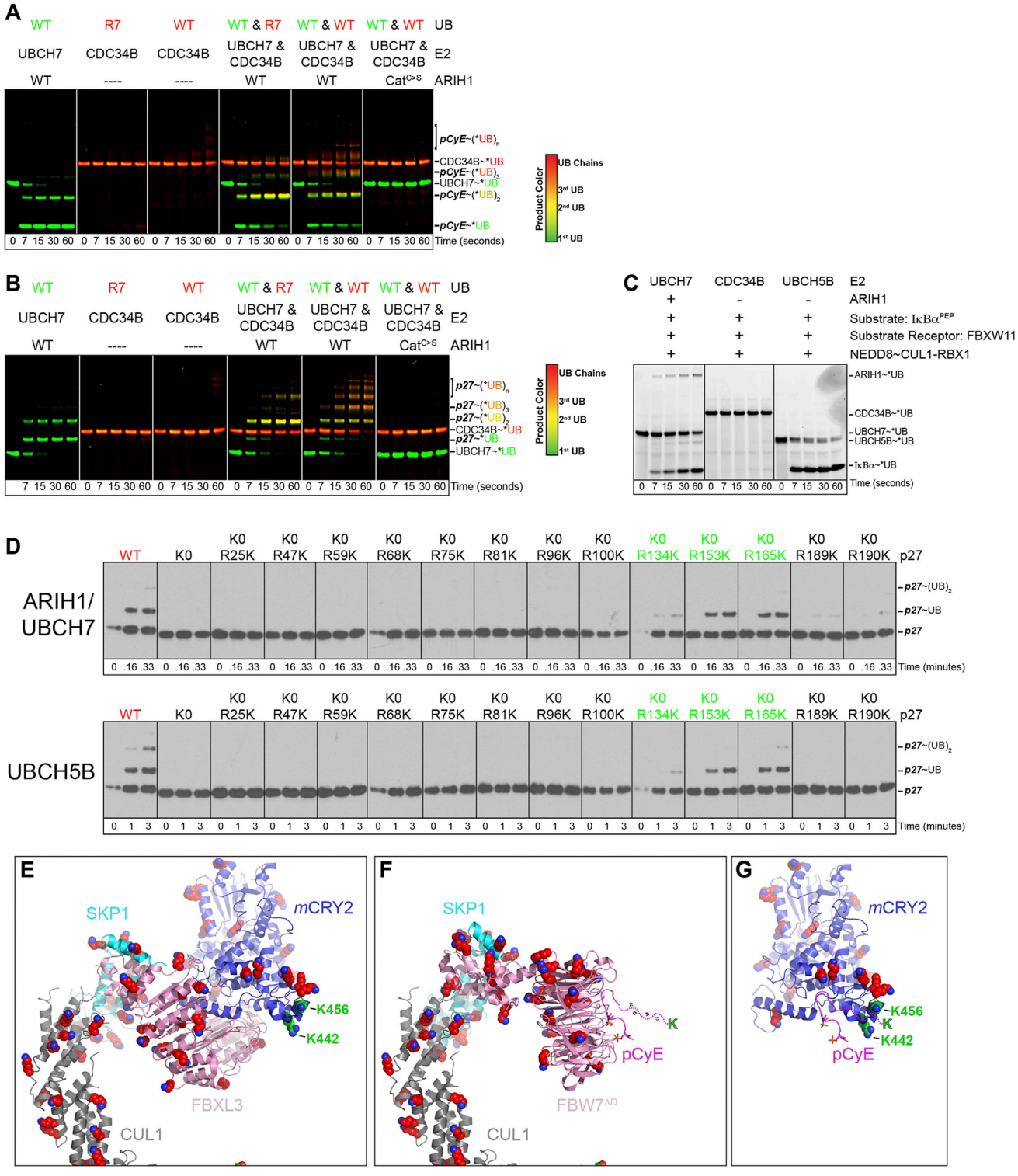

Figure S3. Specificity of UBCH7-ARIH1 Pathway for Mediating Monoubiquitylation of Client Substrates of Neddylated CRLs, Related to Figure 3

(A) The E3 neddylated CRL1$^{FBW7\Delta D}$ and substrate pCyE are in all chase reactions of this dual color pulse-chase assay simultaneously monitoring transfer of "green" (fluorescein-labeled) *UB from UBCH7 via ARIH1 and/or "red" TAMRA-labeled WT or K0 *UB from CDC34 to pCyE.

(B) Same as (A) except with SKP2 (in complex with CKS1) as the substrate receptor and phospho-p27 (in complex with Cyclin A-CDK2) as the substrate.

(legend continued on next page)

(C) Side-by-side comparison of the ARIH1–neddylated CRL (using E2 UBCH7) and canonical CRL–E2 pathway (using E2s UBCH5 and CDC34) for *UB transfer to the SCF^{FBXW11} substrate IκBα.

(D) Comparing target lysine selectivity of ARIH1–neddylated CRL and conventional neddylated CRL RING–E2 mechanism. Anti-p27 Western blots are shown using either WT p27, a lysineless "K0" mutant that is not ubiquitylated, or single lysine variants as indicated. Top, reactions through the UBCH7/ARIH1–neddylated CRL pathway (0-20 s time points) or bottom, through the conventional neddylated CRL RING–UBCH5 pathway (0-3 min time points). Specific lysines are modified in both cases, suggesting that lysine selectivity may involve either intrinsic features of the lysines or their structural location.

(E) Close-up of structure of human SKP1 (cyan)–FBXL3 (pink)– mouse CRY2 (blue) (Xing et al., 2013) modeled on human CUL1 (gray) (Zheng et al., 2002). The mouse CRY2 and human CRY1 sequences are 70.2% identical. Side chains corresponding to lysines in human CUL1, SKP1-FBXL3, and mouse CRY2 are shown in spheres, with the preferred ubiquitylation sites via the ARIH1 pathway (CRY1 K442 and K456, corresponding to mouse R460 and K474) shown in green.

(F) Close-up of structure of human SKP1 (cyan)–$FBW7^{\Delta D}$ (pink)–pCyE (magenta) (Hao et al., 2007) modeled on CUL1 (gray) (Zheng et al., 2002), showing estimated position of the single lysine in the pCyE peptide substrate, which is disordered in the structure.

(G) Superposition of CRL client substrates mCRY2 and pCyE showing their similar spatial location relative to the CUL1–SKP1–F-box portions of the structures.

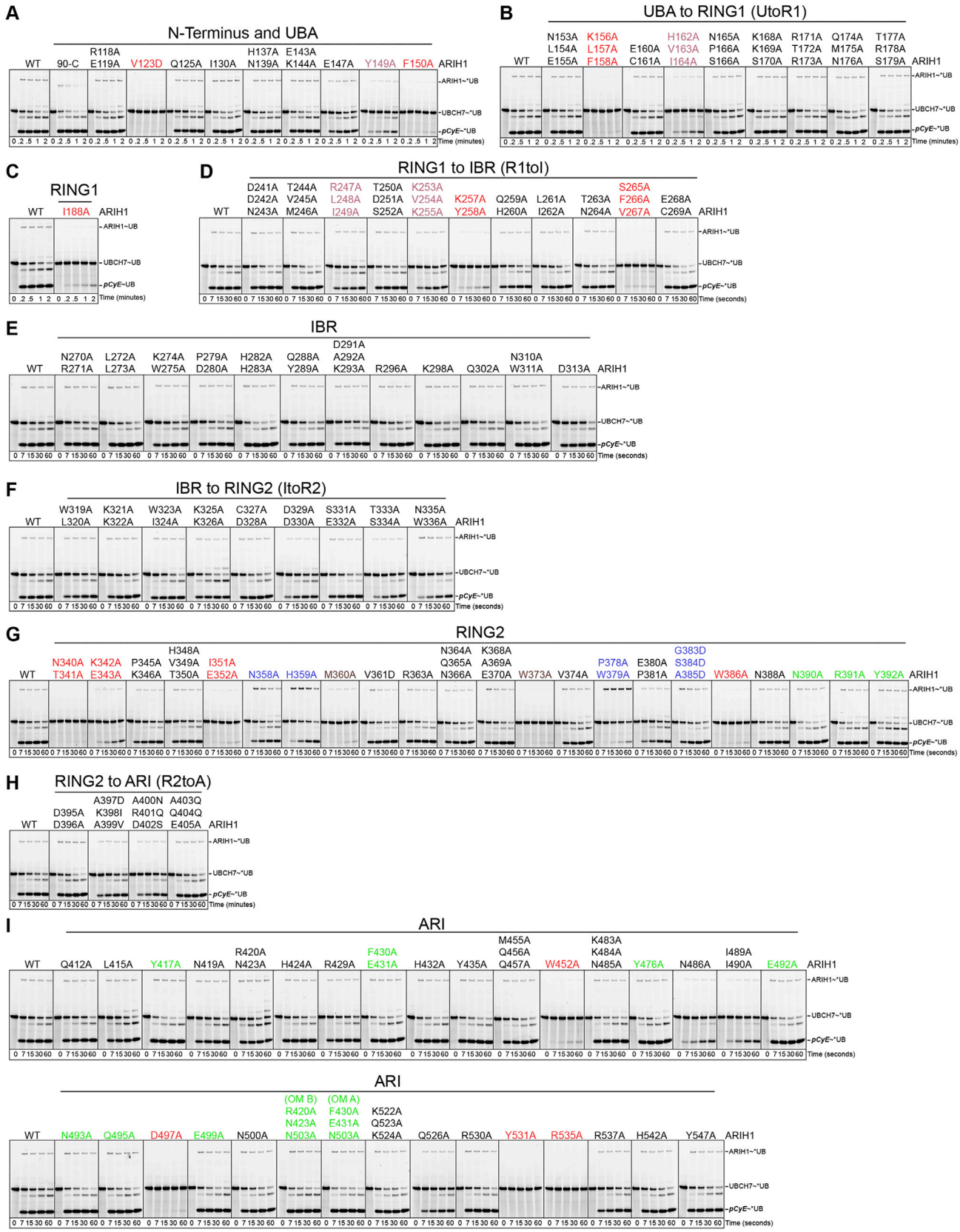

(legend on next page)

Figure S4. Mutational Survey Monitoring Flux through Pathway for Ubiquitylation by ARIH1 Mutants and Neddylated CRL1$^{FBW7\Delta D}$ of Phosphopeptide Substrate Derived from Cyclin E, Related to Figure 4

All chase reactions contain neddylated CRL1$^{FBW7\Delta D}$ and pCyE substrate.

(A) Pulse-chase assay monitoring the transfer of *UB from UBCH7 to pCyE via WT ARIH1 or the indicated mutants from ARIH1's N terminus or UBA domain. Mutants that are categorized as marginally defective and strongly defective are labeled raspberry and red respectively.

(B) Same as (A) but with the indicated mutants from ARIH1's UBA to RING1 linker.

(C) Same as (A) but with the ARIH1 RING1 mutant I188A.

(D) Same as (A) but with the indicated mutants from ARIH1's RING1 to IBR linker region.

(E) Same as (A) but with the indicated mutants from the ARIH1's IBR domain.

(F) Same as (A) but with the indicated mutants from ARIH1's IBR to RING2 linker region.

(G) Same as (A) but with the indicated mutants from ARIH1's RING2 domain. Ligation defective mutants and hyperactive mutants are colored blue and green respectively. Ligation mutants are scored by the appearance and subsequent consumption of the ARIH1∼*UB thioester intermediate, which is typically too transient to observe with WT ARIH1. Hyperactive mutants are scored based on the accelerated consumption of UBCH7∼*UB and ligation to the pCyE substrate. Residues M360 and W373, which are internal to the RING2 fold, are colored brown as their defects likely rise from misfolding of the RING2 domain.

(H) Same as (A) but with the indicated mutants from ARIH1's RING2 to ARI linker.

(I) Same as (A) but with the indicated mutants from ARIH1's ARI domain.

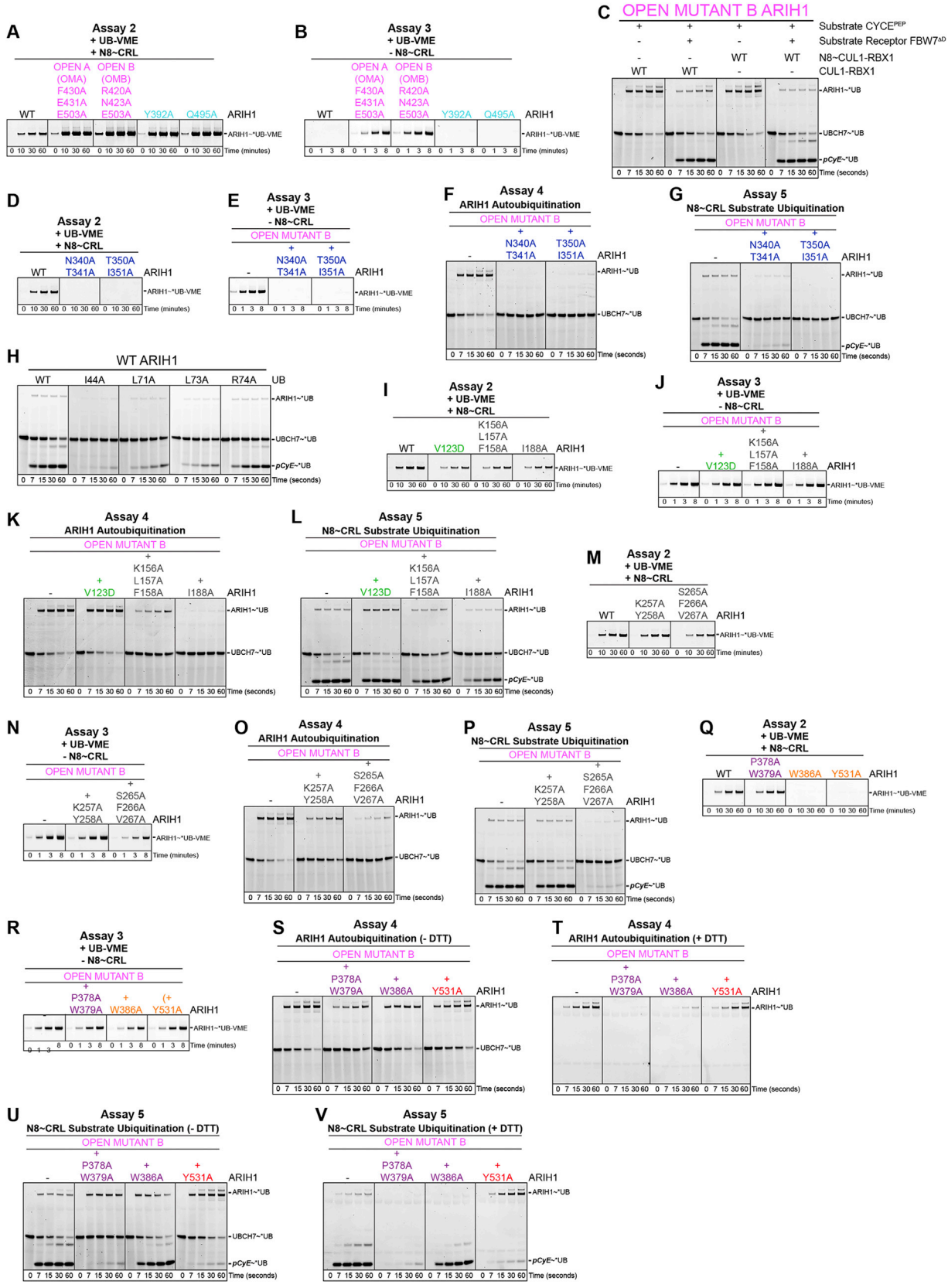

(legend on next page)

Figure S5. Activity Profiling to Assign Signatures to ARIH1 Mutants and Define Roles of ARIH1 Surfaces in Ubiquitylation of CRL Substrates, Related to Figure 5

Representative raw data for mutant versions of ARIH1 subjected to a hierarchy of assays. Activities of a given mutant across the suite of assays constitutes a composite 'Signature Activity Profile,'' which reflects the function(s) of the mutated residue in the ARIH1–neddylated CRL pathway. We identified eight major signatures reflecting different functional roles for the mutated residues.

Assay 1: Test for overall flux through the pathway, shown in Figure 4 and Figure S4.

Assay 2: By comparison to Assay 3, test for neddylated CUL1-RBX1-dependent relief of ARIH1 autoinhibition (i.e., opening the RING2–Ariadne domain intramolecular interactions to expose ARIH1's catalytic Cys357). The experiment monitors reactivity with *UB-VME in the presence of NEDD8∼CUL1-RBX1.

Assay 3: By comparison to Assay 2, test for maintenance of autoinhibition and integrity of RING2 catalytic structure. A collection of hyperactive mutants from Assay 1 and Assay 2 were further tested for reactivity with *UB-VME in the absence of neddylated CUL1-RBX1 to determine if the mutations alone are capable of relieving ARIH1 autoinhibition (termed ''OPEN''), or if they still require neddylated CUL1–RBX1 to relieve autoinhibition. In addition, we selected representative mutants from each individual ARIH1 structural domain that displayed reduced flux through the pathway in Assay 1, and constructed combination mutants that combine both the mutation of interest and OPEN B mutations (R420A N423A E503A) that fully relieve ARIH1 autoinhibition. These combination mutants were assayed for reactivity with *UB-VME in the absence of a neddylated cullin. Defects in reactivity with *UB-VME even when the OPEN mutants were added indicate an intrinsic catalytic defect in RING2, for example in interacting with a UB to be transferred or structure of the active site. Defects in reactivity in the presence of neddylated CUL1–RBX1 (Assay 2), but not in its absence after adding the OPEN mutants (Assay 3), reflect impairment of neddylated CRL-dependent opening of the ARIH1 structure.

Assay 4: Test for intrinsic RBR functions; ability of ARIH1 to receive *UB from UBCH7 independent of neddylated CRL-RBX1 and ARIH1's subsequent ability to mediate intrinsic UB ligation. For all defective mutants, this was examined after adding OPEN mutations B (R420A N423A E503A) to relieve ARIH1 autoinhibition and allow assaying transfer of *UB from *UB∼UBCH7 to ARIH1 in the absence of a neddylated CRL. Persistence of the *UB∼UBCH7 intermediate indicates a defect in intrinsic RBR mechanism of E2-to-RBR E3 UB transfer. Where indicated, if an ARIH1∼UB product was formed, reactions were performed in duplicate and one was quenched with DTT. Whether or not the ARIH1∼*UB product was sensitive to DTT reduction distinguished between accumulation of thioester-linked E3∼UB intermediate or isopeptide-linked automodified ARIH1. Accumulation of the otherwise transient, reducible ARIH1∼*UB intermediate indicates a defect in intrinsic RBR-mediated UB ligation.

Assay 5: In comparison to Assay 4, a defect in Assay 5 but not Assay 4 indicates a specific role in targeting the CRL substrate. After OPEN mutations B (R420A N423A E503A) were added to mutationally relieve ARIH1 autoinhibition, transfer of *UB through the entire UBCH7–ARIH1/neddylated $CRL^{FBW7\Delta D}$ pathway to pCyE substrate was monitored.

(A and B) Assays 2 and 3 for Signature 1, Magenta, defines hyperactive OPEN Mutant, where ARIH1 autoinhibition is disrupted. Signature II, Cyan, defines hyperactive mutant that facilitates neddylated CRL-dependent ''opening'' of ARIH1.

(C) Pulse-chase assay monitoring the transfer of *UB from UBCH7 to pCyE by the hyperactive $ARIH1^{OPEN}$ mutant B, with either nonneddylated or neddylated CUL1-RBX1 and/or the SR $FBW7^{\Delta D}$. This assay tests for the dependence on the SR and/or CUL1 neddylation for targeting the pCyE substrate. While $ARIH1^{OPEN}$ mutant B maintains the requirement for the SR $FBW7^{\Delta D}$ for CRL substrate (pCyE) targeting, mutationally relieving ARIH1 autoinhibition effectively bypasses the requirement for neddylation for targeting the CRL substrate pCyE.

(D–G) Assays 2-5 for Signature III, Blue, defines a role in catalytic UB Binding.

(H) Pulse-chase assay monitoring transfer of *UB or the indicated mutant *UB variants by WT ARIH1 from UBCH7 to pCyE.

(I–P) Assays 2-5 for Signature V, Gray, defines a role in intrinsic RBR function of UB transfer from UBCH7 to RING2.

(I–L) Assays 2-5 for Signature VI, Green, defines a role in neddylated CRL-dependent RBR mechanism of UB transfer from UBCH7 to ARIH1.

(Q–V) Assays 2-5 for Signature IV, Purple defines role in RBR intrinsic ligation. Signature VII, Orange AND Purple, defines dual roles in neddylated CRL-dependent relief of ARIH1 autoinhibition AND in RBR intrinsic ligation. Signature VIII, Orange AND Red, defines dual roles in neddylated CRL-dependent relief of ARIH1 autoinhibition AND in specifically targeting the CRL substrate.

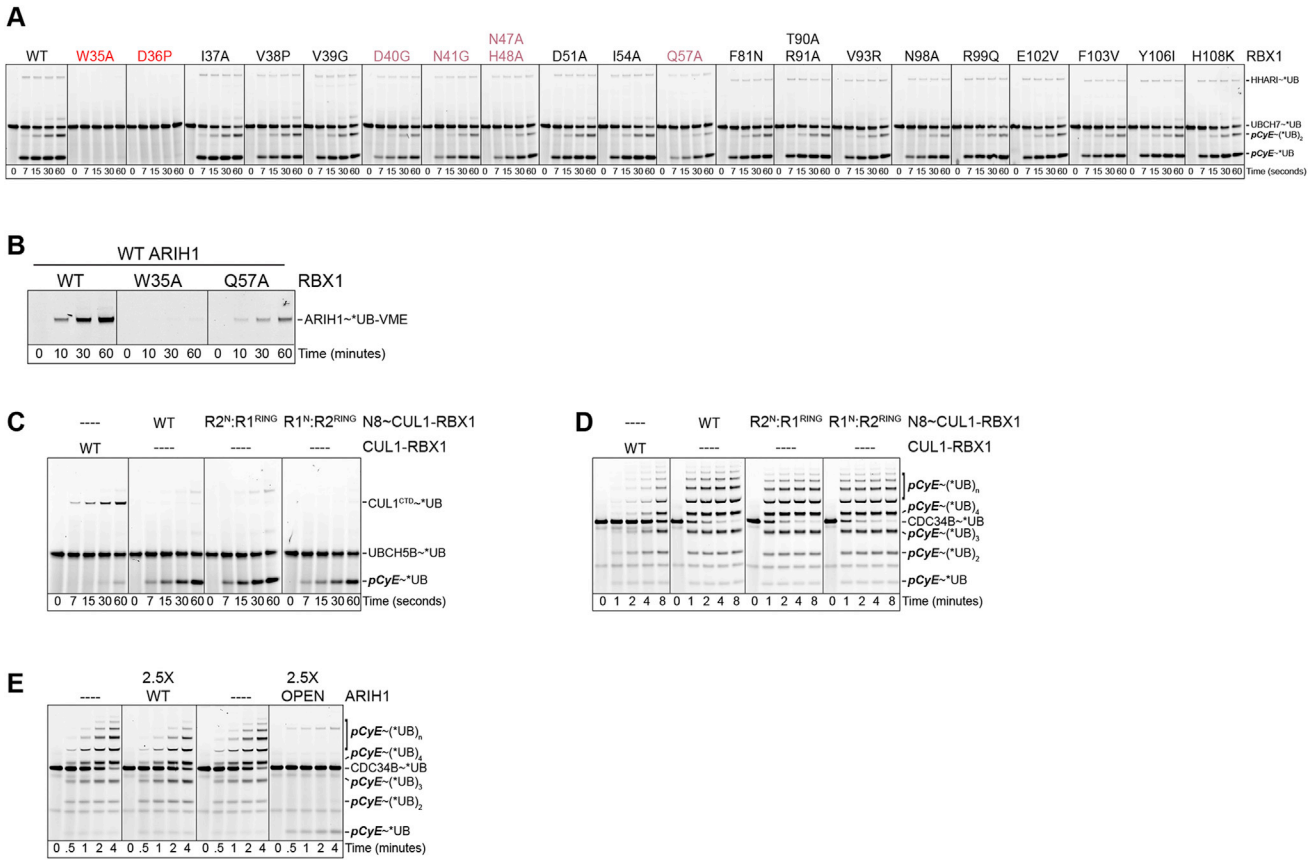

Figure S6. Additional Functions for the RING in Cullin-RING E3 Ligase Activity: RBX1 Residues Modulate ARIH1 Activation and Targeting of Neddylated CRL Substrate, Related to Figure 6

(A) Pulse-chase assay monitoring ARIH1-dependent *UB transfer to pCyE in the presence of the indicated neddylated CUL1–RBX mutants. Coloring is as in Figure S4.

(B) Assay monitoring the reactivity of ARIH1's catalytic cysteine with *UB-VME in the presence of WT or the indicated mutant versions of neddylated CUL1–RBX1.

(C) Test for integrity of RBX1/RBX2 RING swap proteins, by assaying activity through the conventional pathway. Pulse-chase assay to measure the efficiency of *UB transfer to pCyE by UBCH5B with non-neddylated and neddylated WT and the indicated RBX1/RBX2 RING swap proteins. In the absence of neddylation, UBCH5B preferentially transfers *UB to the CUL1 neddylation site (K720) (Duda et al., 2008). Swapping the RBX1 and RBX2 domains has minimal affects on the canonical RING/UBCH5B mechanism of CRL ubiquitylation of pCyE.

(D) Same as (C) except monitoring *UB transfer from CDC34B.

(E) ARIH1^{OPEN} inhibits canonical mechanism of neddylated CRL ubiquitylation with CDC34B. Pulse-chase assay monitoring *UB transfer to pCyE by CDC34 in the absence or presence of a 2.5-fold molar excess of WT or OPEN Mutant A ARIH1.

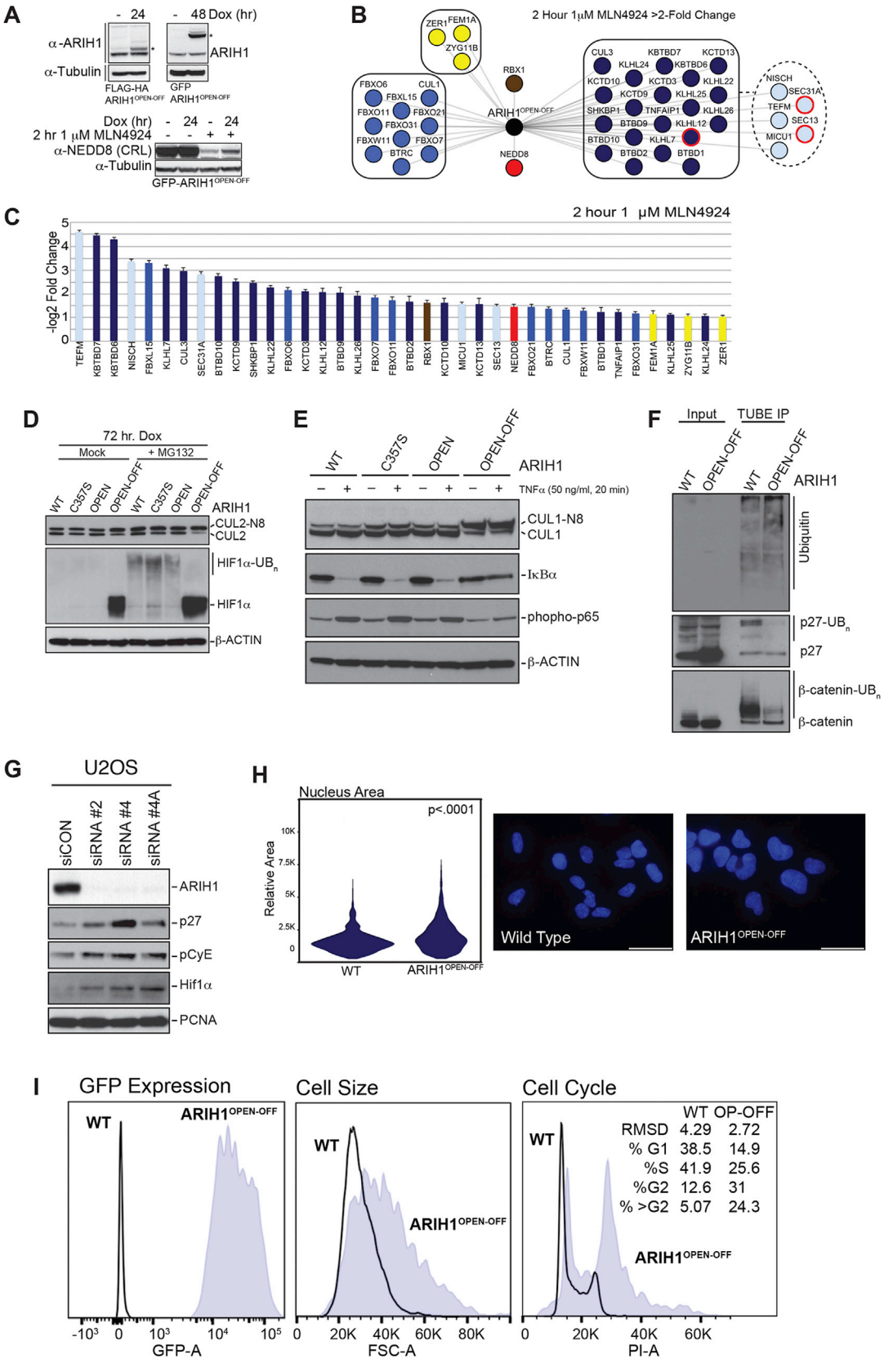

(legend on next page)

Figure S7. Analysis of Cells Overexpressing Dominant-Negative Version of ARIH1: GFP-ARIH1$^{OPEN-OFF}$, Related to Figure 7

(A) Levels of Dox-induced tagged ARIH1$^{OPEN-OFF}$ after 24 hr (FLAG-HA) and 48 hr (GFP). Lower panel: overexpression of GFP-ARIH1$^{OPEN-OFF}$ increases persistence of neddylated cullins after MLN4924 treatment.

(B) Summary of ARIH1$^{OPEN-OFF}$ interactors decreased $\geq$ 2-fold after 2 hr MLN4924 treatment, quantified by TMT AP-MS. CRL1s blue, CRL2s yellow, CRL3s purple, CRL3-associated sky blue, and non-degradative substrate–SR complex (KLHL12–SEC13–SEC31A) highlighted.

(C) Differential ARIH1$^{OPEN-OFF}$ interactors following a 2hr 1 μM MLN4924 treatment. Error bars represent mean $\pm$ SE.

(D-F) The indicated ARIH1 proteins were overexpressed for 72h in 293T cells and cell extracts examined by immunoblotting with the indicated antibodies. In panel F, ubiquitylated proteins were recovered using GST-Tandem UB entities (TUBEs) and immunoblotted for the indicated proteins.

(G) siRNA depletion of ARIH1 increases the levels of of CRL substrates in U2OS cells.

(H) Overexpression of GFP- ARIH1$^{OPEN-OFF}$ results in an increase in nuclear size. Nuclear area was quantified following a 48 hr induction. N = 3739 and N = 3806 nuclei were quantified for GFP-ARIH1$^{OPEN-OFF}$ and No Dox Control, respectively (Student's t test p-value < 0.0001). Scale bar = 35 microns.

(I) Overexpression of ARIH1$^{OPEN-OFF}$ results in cell cycle and cell size defects, as measured by flow cytometry.